Carpathian Journal of Earth and Environmental Sciences, August 2016, Vol. 11, No 2, p. 599 - 608

APPLICATION OF ILLITE CRYSTALLINITY FOR PALEO-TEMPERATURE RECONSTRUCTION: A CASE STUDY IN THE WESTERN SICHUAN BASIN, SW CHINA

Chuanqing ZHU[1], Song RAO[2] & Shengbiao HU[3]

[1]*State Key Laboratory of Petroleum Resources and Prospecting, China University of Petroleum, Beijing 102249, China. Email: zhucq@cup.edu.cn*

[2]*College of Geosciences, Yangtze University, Jingzhou 434023, China. Email: raosong@mail.igcas.ac.cn*

[3]*State Kay Laboratory of Lithospheric Evolution, Institute of Geology and Geophysics, Chinese Academy of Sciences, Beijing 100029, China. Email: sbhu@mail.igcas.ac.cn*

Abstract: The relations of the maximum paleo-geotemperature and vitrinite reflectance with Kübler index (K.I.) of illite crystallinity were characterized, based on the analysis of the K.I. determined by X-ray diffraction (XRD), the maximum paleo-geotemperature reconstructed by apatite fission track (AFT) and vitrinite reflectance (Ro) data. The logarithmic relationship between the maximum paleo-geotemperature and K.I. was revealed: T=-148.95×ln (K.I.)+86.77 (°C); Ro=-3.069×ln (K.I.) +0.068 (%). This relationship has a temperature range of 130~300°C for wide using in geological process, and can be considered as a simple function to convert K.I. to paleo-geotemperature and Ro. This method provides a way for the selection of the thermal history geologic thermometer combination of marine-continental superimposed basin. Comparing to Ro and AFT, the illite crystallinity index is still controversial to be generally used as a maturity and geothermal indicator for the thermal history reconstruction of sedimentary rocks due to the lack of an effective thermal evolution model.

Keywords: Illite crystallinity, X-Ray, Kübler Index, maximum paleo-temperature, Vitrinite reflectance, western Sichuan basin

1. INTRODUCTION

Illite is one of the common clay minerals in sedimentary rocks, and authigenic illite is an important product of the diagenesis and metamorphic evolution of sedimentary rocks. Because illite crystallinity (IC) (Kübler, 1964; 1967) is closely associated with degrees of diagenesis and metamorphism and increases with temperature, it can not only be used to study the diagenesis and very low-grade metamorphism (Zhu, 1995; Arkai et al., 1995; Leoni, 2001; Bi & Mo, 2004) but also serve as a geothermometer to reconstruct thermal history (Francü et al., 1999; Miller & Macdonald, 2004; Klein et al., 2013) or determine the temperature of the present geothermal systems (Browne & Harvey, 1992; Ji & Browne, 2000; Bignall et al., 2001). In a superimposed basin that composed of marine and continental sediments, the marine strata are normally the main source rocks, which have experienced a high degree of thermal evolution but contain rare vitrinite, apatite, and other common paleo-temperature indicators. As a result, it is difficult to identify their maturity and reconstruct their thermal histories (Qin et al., 2009a; 2009b). On the contrary, illite generally exists in all kinds of clay minerals in sedimentary rocks, thus, it may serve as a favorable means to complement the paleo-temperature reconstruction of marine strata.

Estimating paleo-temperatures based on IC can yield relatively accurate results when applied to the burial metamorphism or epimetamorphism stage. However, though the IC-Temperature (Browne & Harvey, 1992; Ji & Browne, 2000), IC-Ro (vitrinite reflectance) relationship (Guthrie et al., 1986; Reinhardt, 1991; Qin et al., 2009a; 2009b) has been studied, but the paleo-temperatures during diagenesis estimated with this method were unsatisfactory. In this study, based on the analysis of the illite crystallinity index K.I. determined by X-ray

diffraction (XRD), the maximum paleo-geotemperature reconstructed by apatite fission track (AFT) and vitrinite reflectance (Ro) data, the relations of the maximum paleo-geotemperature and vitrinite reflectance with Kübler index (K.I.) of illite crystallinity were stated in the western Sichuan basin (Fig. 1), SW China. It has some significance on exploring the equivalence of illite crystallinity and vitrinite reflectance, and establishing the geologic thermometers for thermal history reconstruction in superposition basin.

2. GEOLOGICAL SETTING AND SAMPLING POINTS

The western Sichuan depression is a foreland basin which is bounded by the Longmen Mountain front buried fault to the west and the Longquan Mountain fault to the east (Wang, 1997; Li et al., 2011). Before the Indosinian orogeny in the late Triassic (T_3), the western Sichuan region was at the western boundary of the upper Yangtze Cratonic basin, collectively forming a continental platform composed of carbonate rock (Zhu & Liang, 2001; Li et al., 2011). As the Longmen Mountain and Daba Mountain orogenic belts developed during the Indosinian orogeny, continental sedimentation initiated in this area. An ultra-thick Upper Triassic series composed primarily of lithic sandstone formed when voluminous clasts were deposited. Longmen Mountain has been thrust onto the western Sichuan depression several times since the Indosinian orogeny began, resulting in regional faults and the uplift and denudation of the basin margins. The Indian Plate then collided with the Eurasian Plate during the Himalayan orogeny, inducing more violent thrusting of Longmen Mountain. These structural events created the Longmen Mountain thrust belt and the foreland basin in western Sichuan (Wang, 1997; Li et al., 2011). The boreholes in the western Sichuan depression, such as CY92 and CY95, were drilled in the upper continental petroleum system in T_3-J_3. The illite samples are mainly from the mudstone and shale core rocks of the borehole CY 95 (Fig. 1).

3. EXPERIMENT

The illite crystallinity was analysed by X-ray diffraction (XRD) in the Geological Experiment Research Centre, Research Institute of Petroleum Exploration & Development. In the sample preparation process (Yang, 1993; You et al., 2007), it must be eliminated inherited terrigenous clastic illite and choose the illite from the authigenic origin and diagenesis stage or their low rank metamorphism.

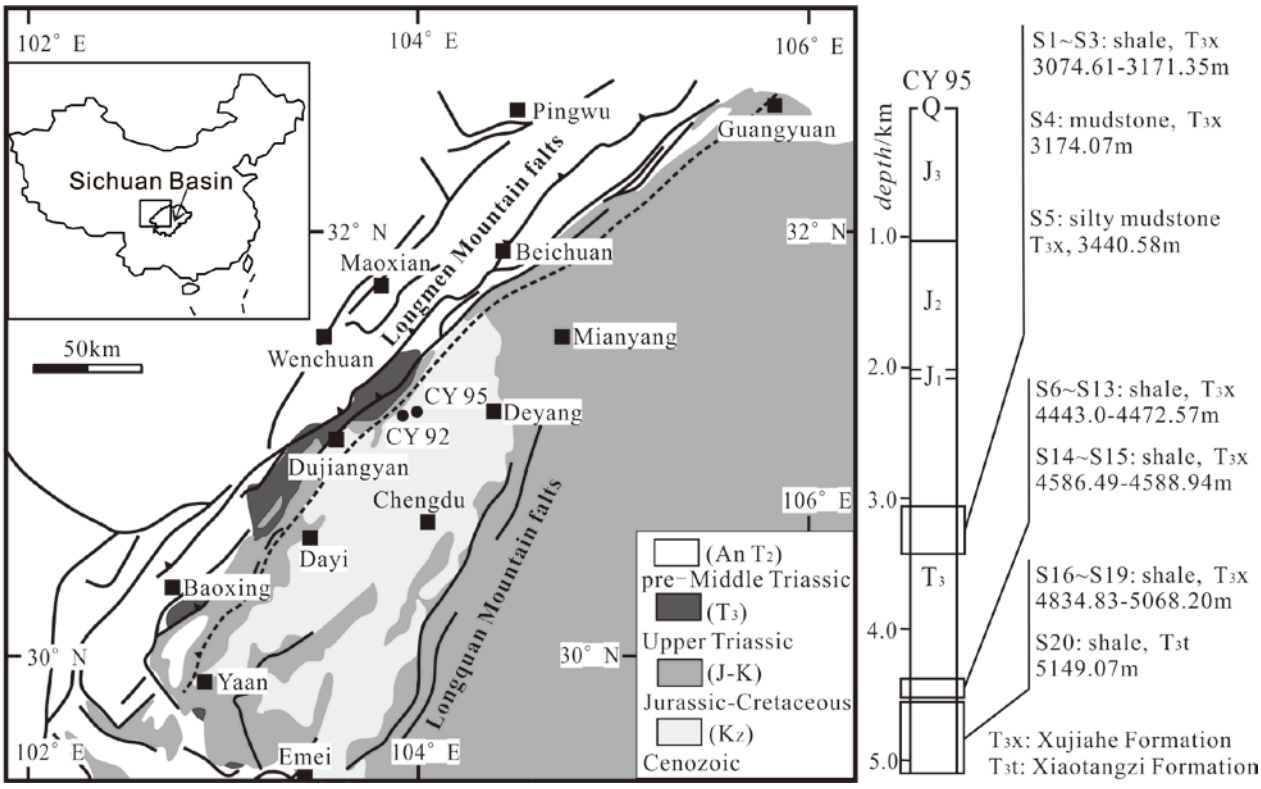

Figure 1. Geological map of the western Sichuan basin and the sampling points

The experimental steps: (1) weigh 40 mg clay with less than 2 μm grain size, put the sample in a 10 ml test tube, and add 0.7 ml distilled water; (2) vibrate it into suspension with ultrasonic wave, and drop it on clean slides; (3) each sample shall be made into two directional pieces for being dried by natural air and measured.

The adopted instruments are D/max-2500 X diffractometer produced by Rigaku with a Cu-Ka1 ray of wavelength, the pipe pressure and flux are respectively 40 kV and 100 mA. The scanning speed is 2°/min, and the slit system is 1°, 1°, 0.3 mm, scanning range is 216°-35°, 2 times repeated scanning. The MD I Jade 5.0 software package is used for data processing, when measuring illite crystallinity of K.I., it shall firstly determine the background line, and then measure the full width at half maximum (FWHM) of 10 Å diffraction peak (Wang, 1998; Wang et al., 2000; You et al., 2007), as shown in figure 2. Figure 3 shows the X-ray patterns of illite at different depths of borehole CY 95.

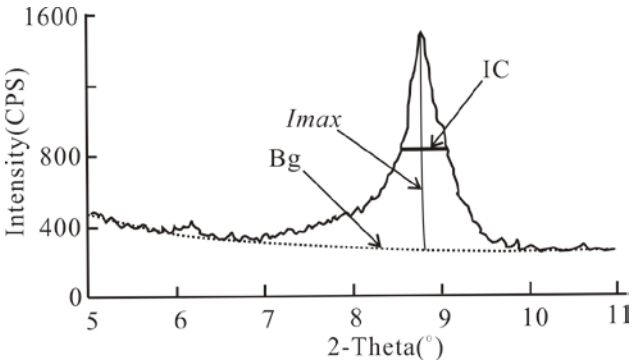

Figure 2. The measurement of Kübler Index of illite crystallinity (after Wang et al., 2000)
Bg- Background Line; Imax- maximum intensity; IC- Kübler Index of illite crystallinity

4. RESULT AND DISCUSSION

4.1 Result

Kübler Index is actually based on the Scherrer's equation (Scherrer, 1918), therefore, with the increase of the index, the diffraction peaks become wider and crystallinity worse. In order to reduce the effects of sample preparation, instrument conditions, and methods of testing differences on test result and improve data comparability, the data should be calibrated with the international standard sample in the process of measuring Kübler index (You et al., 2007). The calibrated K.I. data are presented in table 1a, along with the increase of the depth, Kübler index on the whole show decreasing trend, reflecting illite crystallinity increase with the sample buried depth.

4.2 Discussion

Some researchers have reported their findings regarding the relationship between crystallinity and the generation temperature of illite and the division of diagenesis to the very low-grade metamorphism process. During the telodiagenesis stage (corresponding to the high-grade diagenetic zone), the K.I. for illite crystallinity varies from 1.0 to 0.42 (°Δ2θ) and the temperature cap is 200°C (when K.I.=0.42 (°Δ2θ), T= ~200°C). During burial metamorphism, the K.I. is between 0.25 and 0.42 (°Δ2θ), and the temperature is between 200°C and 300°C (when K.I.=0.25(°Δ2θ), T= ~300°C). During epimetamorphism, which corresponds to the greenschist facies, the K.I. is smaller than 0.25(°Δ2θ), and the temperature is higher than 300°C (Kübler, 1964; Arkai et al., 1995; Bi & Mo, 2004).

In light of the division of diagenesis in metamorphism processes, the K.I. values of illite in CY95 and the maximum paleo-temperatures attained at different depths were estimated using the data in previous reports (Qin et al., 2009b; Hu et al., 2012), at a depth of ~4080 m, the K.I. is ca. 0.60 (°Δ2θ), and the maximum paleo-temperature was ca.150°C. The CY 95 well is adjacent to CY 92, with the same geological background, similar geologic structure and sedimentary evolution history, so according to the constrained point (T=ca. 150°C, at ca.4000m) and reference of palaeogeothermal gradients of CY 92 well, the maximum paleo-geotemperature profiles can be established.

Figure 4 shows the AFT modelling result of CY92-1 (at a depth of 2142m).

In CY92-1 (at 2142 m deep), the central AFT age was 42.3±3.0 Ma, and the average track length was 11.76±0.26μm. The modelling result revealed that CY92-1 reached a maximum paleo-temperature of approximately 115-130°C when it was buried at a maximum depth at ca.60Ma.

Figure 5 displays both the maximum paleo-geotemperature profile of CY92 that was reconstructed based on Ro and AFT, and the maximum paleo-temperature profile of CY95.

The maximum paleo-temperature profiles of the two boreholes intersect with the line of depth=0 (namely, the earth's surface) when T1=~72°C and T2=~54°C, respectively. Given the geothermal gradient, ~26°C /km, a temperature difference of

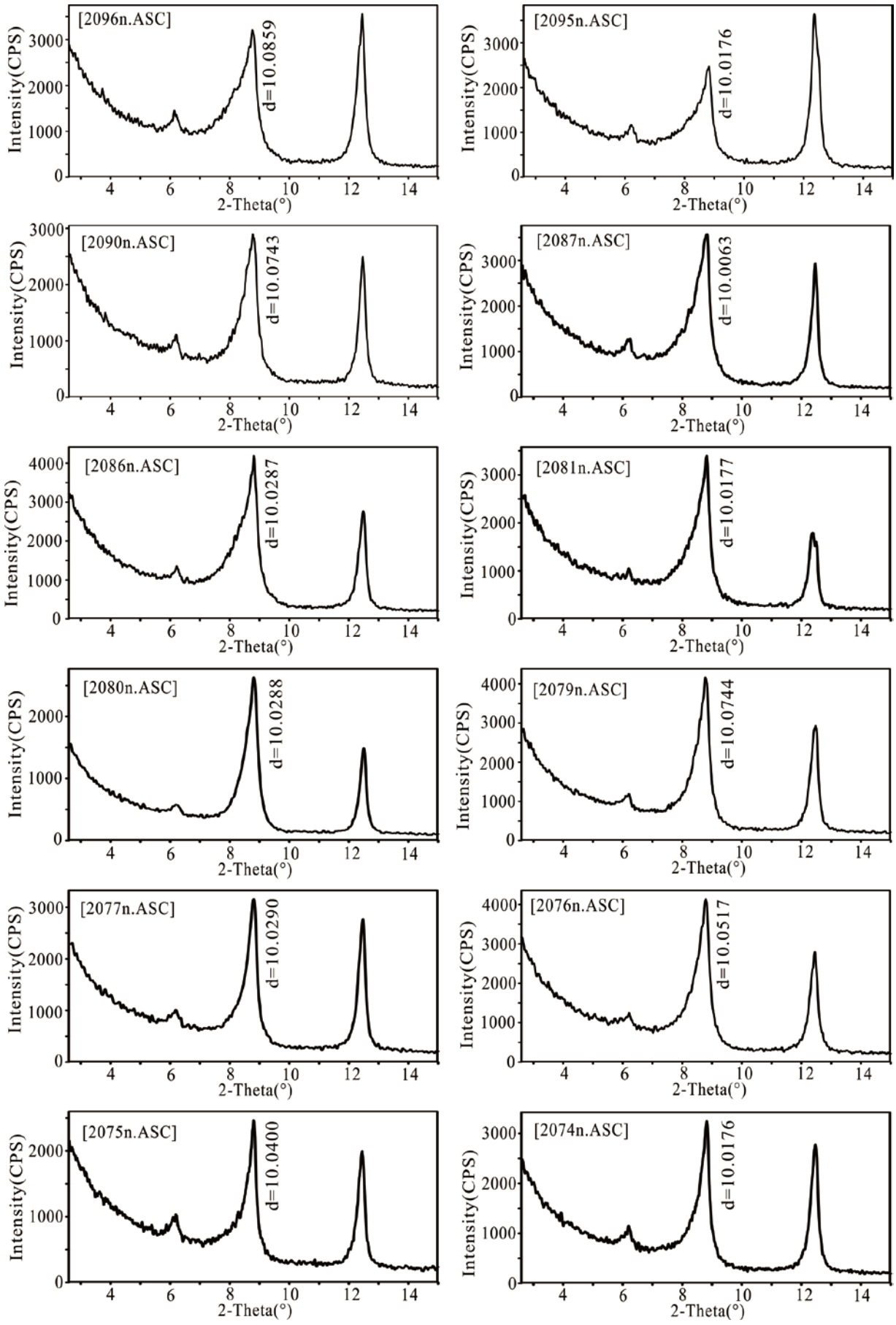

Figure 3. X-ray patterns of illite at different depths of borehole CY 95

Table 1. The illite K.I. data of borehole CY 95 samples in the western Sichuan basin (a) the maximum temperature and the calculated Ro of the samples (b)

a. **b.**

Sample No.	Test No.	Depth (m)	Strata	Lithology	K.I.$_{measured}$ (K.I.)	K.I. $_{calibrated}$ (K.I.)		Maximum T (°C)	Ro (%)
S1	2096	3074.61	T_3x^5	shale	0.66	0.68		133.94	1.05
S2	2095	3163.21	T_3x^5	shale	0.67	0.69		136.24	1.09
S3	2093	3171.35	T_3x^5	shale	-	-		-	-
S4	2092	3174.07	T_3x^5	mudstone	-	-		-	-
S5	2090	3440.58	T_3x^4	mudstone	0.60	0.62		143.46	1.24
S6	2088	4443.00	T_3x^3	shale	-	-			
S7	2087	4444.25	T_3x^3	shale	0.61	0.63		169.55	1.77
S8	2086	4446.75	T_3x^3	shale	0.59	0.61		169.62	1.77
S9	2085	4463.90	T_3x^3	shale	-	-		-	-
S10	2084	4465.18	T_3x^3	shale	-	-		-	-
S11	2083	4467.48	T_3x^3	shale	-	-		-	-
S12	2082	4470.31	T_3x^3	shale	-	-		-	-
S13	2081	4472.57	T_3x^3	shale	0.62	0.64		170.29	1.77
S14	2080	4586.49	T_3x^2	shale	0.50	0.52		173.25	1.85
S15	2079	4588.94	T_3x^2	shale	0.51	0.53		173.31	1.85
S16	2077	4834.83	T_3x^2	shale	0.51	0.53		179.71	1.98
S17	2078	4836.31	T_3x^2	shale	-	-		-	-
S18	2076	4942.02	T_3x^2	shale	0.54	0.56		182.49	2.04
S19	2075	5068.20	T_3x^2	shale	0.52	0.54		185.77	2.11
S20	2074	5149.07	T_3t	shale	0.50	0.52		187.88	2.17

***Note:** (a) K.I. data, the data was tested in the Research Institute of Petroleum Exploration & Development, Petrol China. The K.I. data have been calibrated by using international standards: K.I.$_{calibrated}$ = 0.977×K.I.$_{measured}$+ 0.0336(°Δ2θ), R^2 = 0.9835 (You, et al., 2007). (b) Maximum temperature and modelled Ro calculated by using EASY%Ro model (Sweeney & Burnham, 1990).

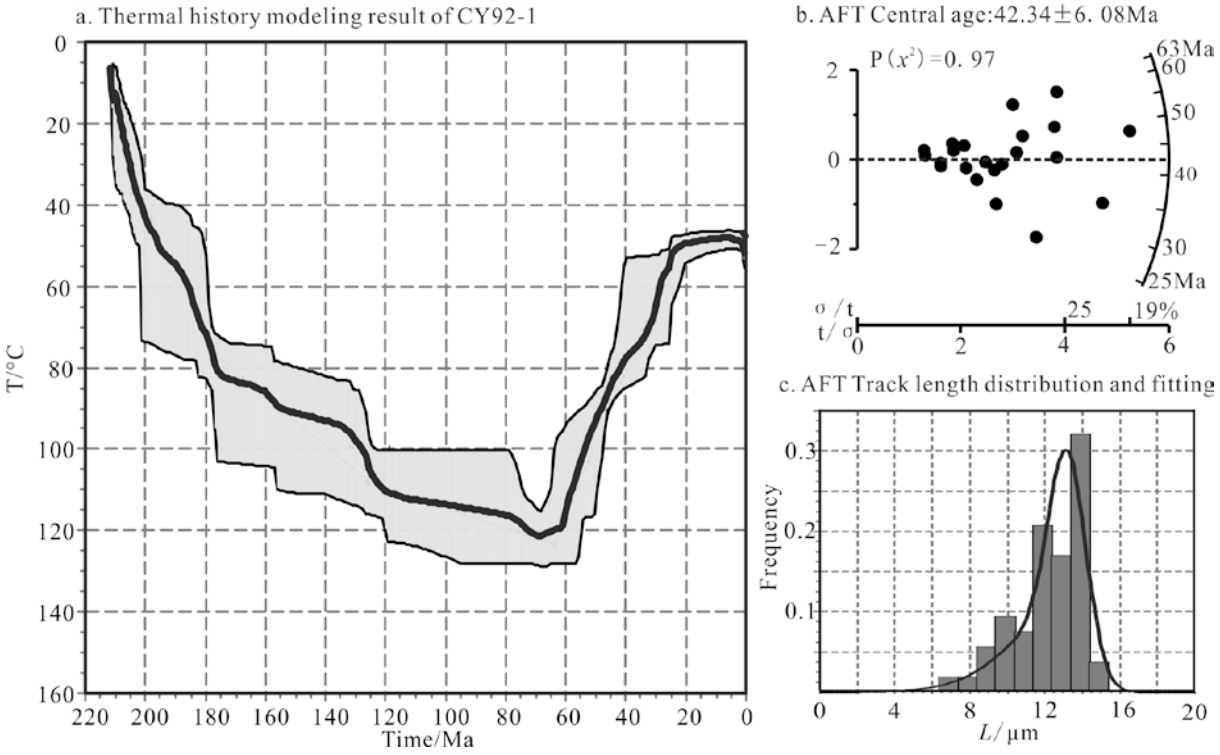

Figure 4. AFT thermal history modeling result of CY92-1

10000 paths have been modelled using Monte Carlo method. The inversion results are a series of possible or equivalent thermal history paths, and these possible thermal history paths constitute a probability-distribution belt, a more complex thermal history exhibits a wider distribution belt and greater uncertainty. The light grey regions indicate the envelopes of "good traces" (0.6≤GOF≤1.0) and the black bold line in each result indicates the mean trace.

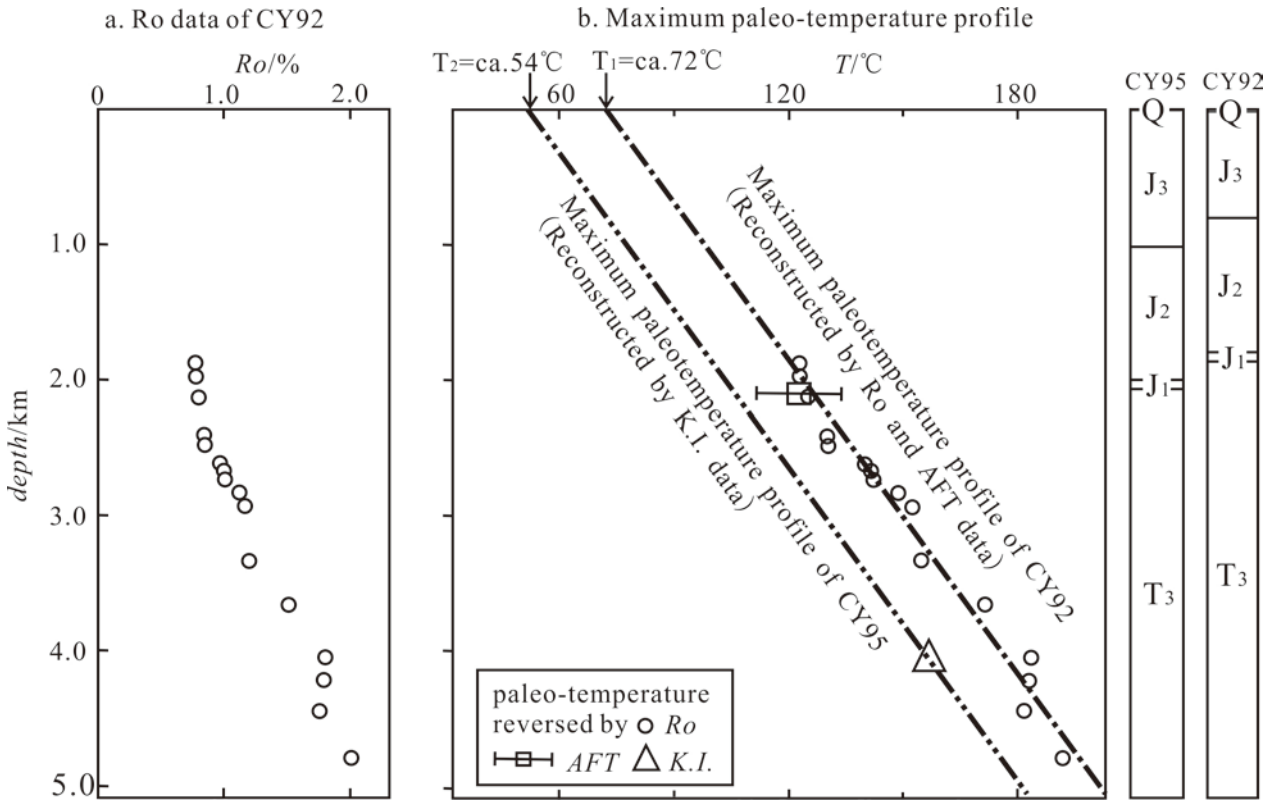

Figure 5. Paleo-temperature reconstruction of borehole CY 92 and CY 95. The maximum paleo-temperature profile of CY 92 was reconstructed by the Ro data (a) and the AFT data of sample CY 92-1 (see Fig.4). The paleo-temperature modelling of Ro data based on the EASY%Ro model (Sweeney & Burnham, 1990).

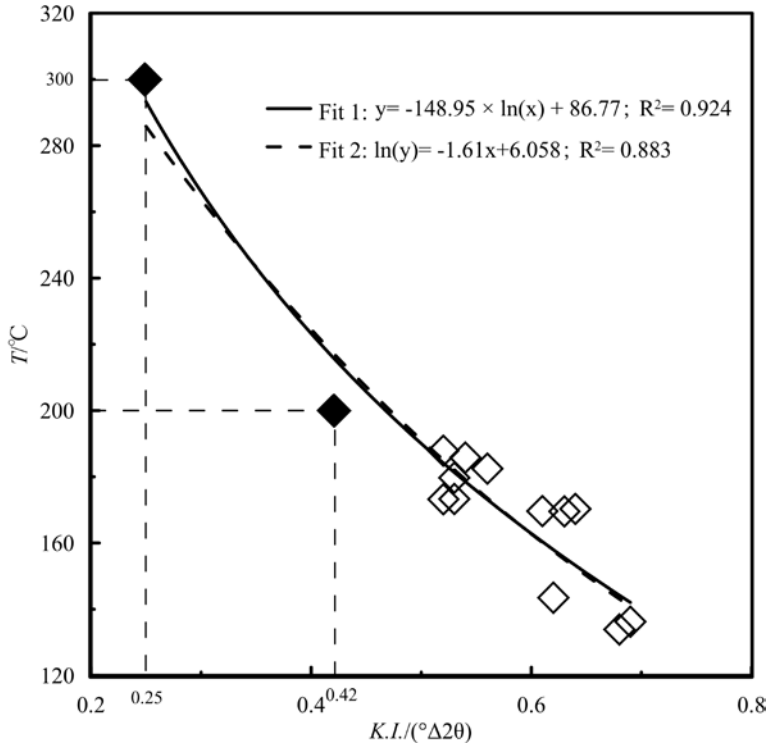

Figure 6. Correlation between the K.I. data and the maximum paleo-temperatures of borehole CY 95

approximately 18°C could indicate a difference of ~690 m in the thickness of removed sediments, it can be assumed that this area has undergone continuous cooling, uplift, and denudation since ~60Ma, which resulted in a geothermal gradient reduction from ~26°C /km to ~22°C /km and the

removal of ~1.3 to 1.9 km of sediments.

The relationship of CY 95 well illite crystallinity Kübler index and temperature was as shown in figure 6 and Table 1b, which has a good logarithmic relationship:

$T=-148.95\times\ln(K.I.)+86.77$ (°C), ($R^2=0.924$) (1)

Similar to Ro, the illite crystallinity is not only related with the maximum paleo-geotemperature, but also with the duration. But their evolution properties vary with temperature and time may not be completely consistent. In order to explore the relationship between K.I. and Ro, we put forward Ro value (see table 1b) of the sample according to the maximum paleo-geotemperature of CY 95 well that reflects a good logarithmic relationship between the two (see Fig. 7, the forward Ro modelling examples see Fig. 8):

$Ro=-3.069\times\ln(K.I.)+0.068$ (%), ($R^2=0.927$) (2)

Estimating paleo-temperatures based on K.I. can yield relatively accurate results when applied to the burial metamorphism or epimetamorphism stage. However, though the IC-Temperature, IC-Ro relationship (Guthrie et al., 1986; Qin et al., 2009a; 2009b) has been studied, the paleo-temperatures during diagenesis stage (K.I.>0.42(°Δ2θ)) estimated with this method were unsatisfactory.

In this study, the results of thermal history for the entire geologic thermometer have good consistency, and after the mark points K.I. =0.42(°Δ2θ) and K.I.=0.25(°Δ2θ) are introduced as a constraint into the fitting function (in Fig. 6 and Fig. 7, the blank rhombuses indicate the actual data, while the black rhombuses indicate 2 theoretical points (K.I.=0.42(°Δ2θ), 0.25(°Δ2θ)); a better fitting degree can still be got. Therefore, formula (1) and (2) can be considered as a simple function to convert K.I. to paleo-geotemperature and Ro. However, the thermal evolution model of the IC has not been stated, it needs further works on the combination of the K.I. and other temperature indicators (Guthrie et al., 1986; Reinhardt, 1991; Wyld & Copeland, 2003; Qin et al., 2009a; 2009b; Zhu et al., 2015) to reveal their correlations.

5. CONCLUSIONS

The corresponding relationships of the illite crystallinity index K.I. determined by X-ray diffraction (XRD), the maximum paleo-geotemperature and Ro value have been discussed, and the good logarithmic relationships between the maximum paleo-geotemperature, the Ro value with K.I. were obtained. The relationships has a temperature range of 130~300℃ for wide using in many geological processes, for example, in the marine strata that lack of vitrinite reflectance, the stratum maximum paleo-geotemperature and the maturity of organic matter can be estimated by K.I.. This method provides a way for the selection of the

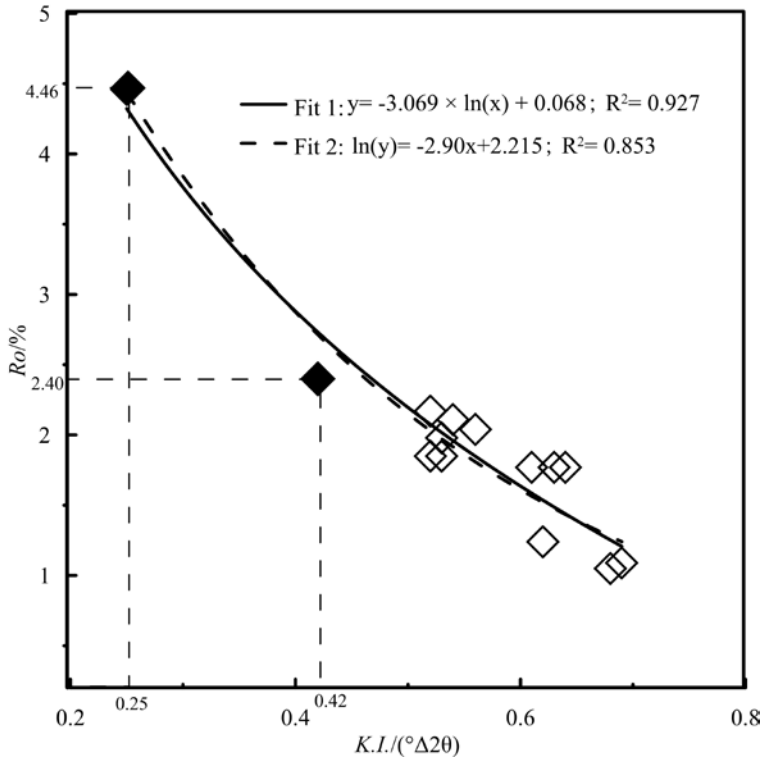

Figure 7. Correlation between the K.I. data and the modelled Ro data

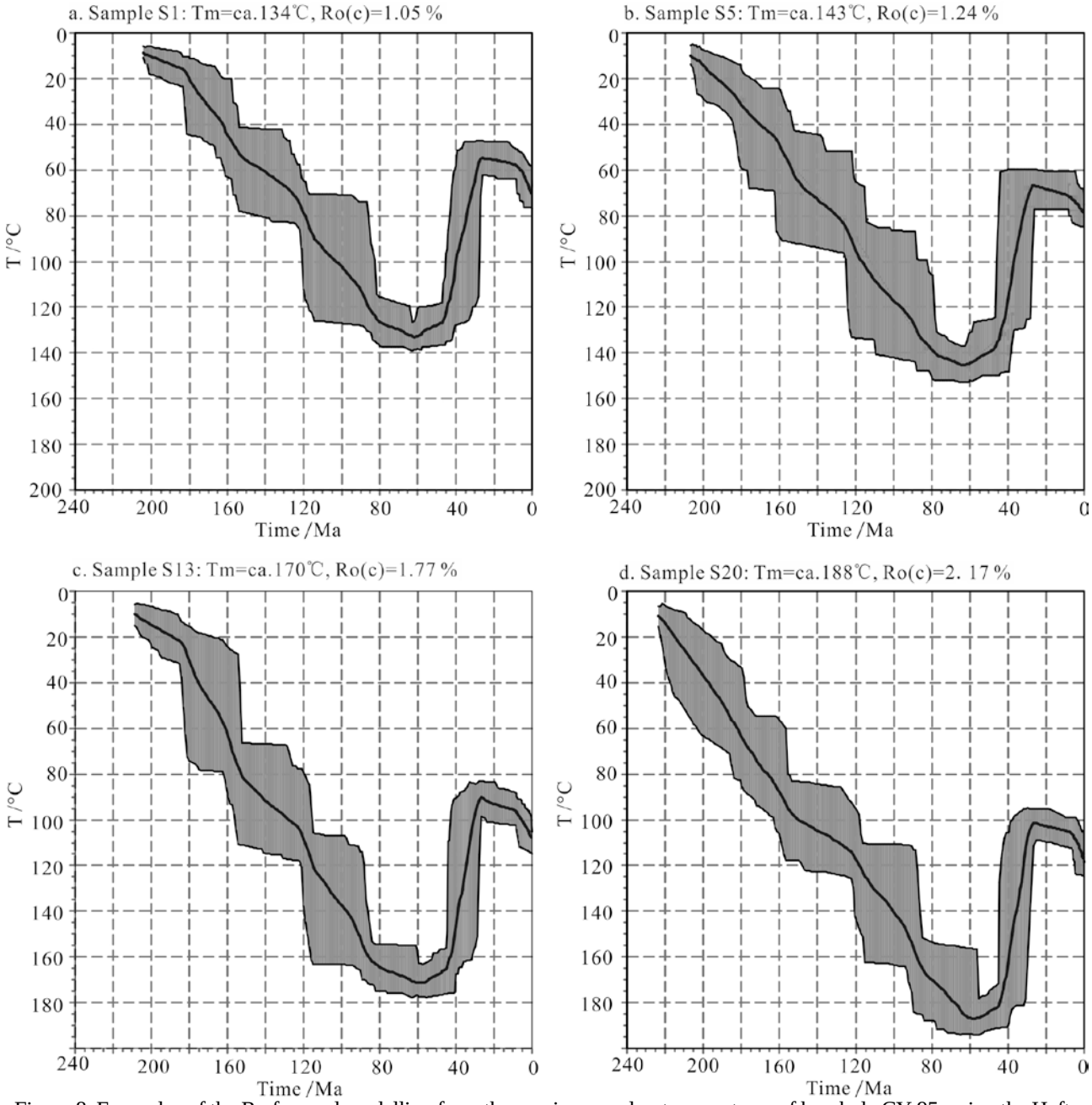

Figure 8. Examples of the Ro forward modelling from the maximum paleo-temperatures of borehole CY 95, using the Hefty 1.7.4 software package (Ketcham, et al., 2007) based on the EASY%Ro model (Sweeney & Burnham, 1990). The dark grey regions indicate the envelopes of "good traces" (0.8≤GOF≤1.0) and the black bold line in each result indicates the mean trace.

thermal history geologic thermometer combination of marine-continental superimposed basin.

However, unlike Ro and AFT, the illite crystallinity index is still controversial due to the lack of an effective thermal evolution model, and more research is therefore necessary before it can be generally used as a maturity and geothermal indicator for the thermal history reconstruction of sedimentary rocks.

Acknowledgements

This study was supported by the National Key Basic Research Development Plan of China ("973" Projects) (2012CB214703) and the National Science Foundation of China (41102152). We would like to acknowledge the helpful comments from the reviewers and the suggestions provided by the editors.

REFERENCES

Arkai, P., Sassi, F. P. & Sassi, R. 1995. *Simultaneous measurements of chlorite and illite crystallinity; a more reliable tool for monitoring low-to very low grade metamorphisms in metapelites: a case study from the Southern Alps (NE Italy).* European Journal of Mineralogy, 7:1115-1128.

Bi, X. M. & Mo, X. X. 2004. *Transition from diagenesis to low-grade metamorphism and related minerals and energy resources*. Earth Science Frontiers, 11: 287-294.

Bignall, G., Tsuchiya, N. & Browne, P. R. L. 2001. *Use of illite crystallinity as a temperature indicator in the Orakei Korako geothermal system, New Zealand*. Transactions-Geothermal Resources Council, 25: 339-344.

Browne, C. M. & Harvey, C. C. 1992. *Crystallinity of subsurface clay minerals in the TeMihi Sector of the Wairakei geothermal system, New Zealand*. 14th New Zealand geothermal Workshop, 267-272.

Francü, E., Francü, J. & Kalvoda, J. 1999. *Illite crystallinity and vitrinite reflectance in Paleozoic siliciclastics in the SE Bohemian Massif as evidence of thermal history*. Geologica Carpathica, 50: 365-372.

Guthrie, G. M., Houseknecht, D. W. & Johns, W. D. 1986. *Relationships among vitrinite reflectance, illite crystallinity, and organic geochemistry in Carboniferous strata, Ouachita mountains, Oklahoma and Arkansas*. AAPG bulletin, 70: 26-33.

Hu, D. Q., Han, C. Y., Ma, R., Liu Y., Wang, J. & Gao, Z. H. 2012. *The very low grade metamorphism in the Upper Paleozoic in Xinlingol area of Inner Mongolia, NE China: Evidence from studies of illite and vitrinite reflectance*. Acta petrologica sinica, 28: 3042-3049.

Ji, J. & Browne, P. R. L. 2000. *Relationship between illite crystallinity and temperature in active geothermal systems of New Zealand*. Clay and Clay Minerals, 48: 139-144.

Ketcham, R. A., Carter, A. C., Donelick, R. A., Barbarand, J. & Hurford, A. J. 2007. I*mproved modeling of fission-track annealing in apatite*. Am. Mineral., 92: 799-810.

Klein, T., Craddock, J. P. & Zulauf, G. 2013. *Constraints on the geodynamical evolution of Crete: insights from illite crystallinity, Raman spectroscopy and calcite twinning above and below the 'Cretan detachment'*. International Journal of Earth Sciences, 102: 139-182.

Kübler, B. 1964. *Les argiles, indicateurs de met amorphisme*. Pev Ftist Franc Petro, 19:1093- 1112.

Kübler, B. 1967. *La cyrstallinite de I'illite et les zones tout a fait superieures du metamorphism*. In: Etages tectnoiques, Colloque de Neuehatel, pp. 105-121.

Leoni, L. 2001. *New standardized illite crystallinity data from low- to very-low grade metamorphic rocks (Northern Apennines, Italy)*. European Journal of Mineralogy, 13:1109-1118.

Li, Z. W., Liu, S. G., Chen, H. D., Sun, D. , Lin, J. & Tang, C. 2011. *Structural superimposition and conjunction and its effects on hydrocarbon accumulation in the Western Sichuan Depression*. Petroleum Exploration and Development, 38: 538-551.

Miller, S. & Macdonald, D. I. M.2004. *Metamorphic and thermal history of a fore-arc basin: the Fossil Bluff Group, Alexander Island, Antarctica*. Journal of Petrology, 45: 1453-1465.

Qin, J. Z., Li, Z. M. & Teng, G. 2009a. *A study on paleo-geothermometer of high mature marine sequences in South China*. Oil & Gas Geology, 30: 608-618.

Qin, J. Z., Teng, G., Yang, Q. & Shen, B. J. 2009b. *Research on maturity indicators of high-maturity marine strata in the eastern Sichuan Basin*. Acta Petrolei Sinica, 30: 208-213.

Reinhardt, M. 1991. *Vitrinite reflectance, illite crystallinity and tectonics: results from the Northern Apennines (Italy)*. Organic Geochemistry, 17: 175-184.

Scherrer, P. 1918. *Bestimmung der Grösse und der inneren Struktur von Kolloidteilchen mittels Röntgenstrahlen*. Mathematisch-Physikalische Klasse, 2: 98-100.

Sweeney, J. J. & Burnham, A. K., 1990. *Evaluation of a simple model of vitrinite reflectance based on chemical kinetics*. AAPG Bulletin, 74: 1559-1570.

Wang, H. J. 1998. *On the error calculation of the Kübler index of i1lite crystallinity*. Geological review, 44: 328-335.

Wang, H. J., Tao, X. F. & Rahn, M. 2007. *Some aspects of illite crystallinity and its applications in low temperature metamorphism*. Earth Science Frontiers, 14: 151-156.

Wang, H. J., Zhu, M. X., Xu, Q. S., Liu, C. X. & Bian, Z. H. 2000. *Relationship between slit system and the Kübler index of illite crystal1inity and discussion on relevant problems*. Geological review, 46: 588-593.

Wang, T. Z. 1997. *Significance of longmenshan thrust in evolution and oil-gas exploration of western Sichuan basin*. Geoscience, 11: 496-500.

Wyld, J. & Copeland, P. 2003. *Metamorphic Evolution of the Luning-Fencemaker Fold-Thrust Belt, Nevada: Illite Crystallinity, Metamorphic Petrology, and40Ar/39Ar Geochronology*. Journal of Geology, 111:17-38.

Yang, X. Z. 1993. *Illite crystallinity and its geological significances*. Acta Sedimentologica Sinaca, 11: 92-98.

You, J. C., Bi, X. M. & Hou, C. M. 2007. *Calibration of illite crystallinity measurements by using international standards and its significance*. Geosciences, 22:53-58, 2008.

Zhu, C. Q., Qiu, N. S., Jiang, Q., Hu, S. B. & Zhang, S. 2015. *Thermal history reconstruction based on multiple paleo-thermal records of the Yazihe area, western Sichuan depression.* Chinese Journal of Geophysics, 58: 3660-3670.

Zhu, G. 1995. *Grading the extreme-low metamorphic clastic sedimentary rocks by the crystallinity of the illite*. Petroleum exploration and development, 22: 33-34.

Zhu, T. & Liang, E. Y. 2001. *Discussion on oil and gas exploration of Xujiahe group in Yazi River structure of the middle Longmenshan in western Sichuan*. Journal of Chengdu University of Technology, 28:59-63.

Received at: 12. 04. 2016
Revised at: 14. 06. 2016
Accepted for publication at: 24. 06. 2016
Published online at: 04. 07. 2016